Asymmetry index in muscle activations

Asymmetry index in muscle activations

C. Castagneri, V. Agostini, S. Rosati, G. Balestra, *Member, IEEE,* and M. Knaflitz, *Member, IEEE*

***Abstract*—Gait asymmetry is typically evaluated using spatio-temporal or joint kinematics parameters. Only a few studies addressed the problem of defining an asymmetry index directly based on muscle activity, extracting parameters from surface electromyography (sEMG) signals. Moreover, no studies used the extraction of the muscle *principal activations* (activations that are necessary for accomplishing a specific motor task) as the base to construct an asymmetry index, less affected by the variability of sEMG patterns. The aim of this study is to define a robust index to quantitative assess the asymmetry of muscle activations during locomotion, based on the extraction of the principal activations. SEMG signals were analyzed combining Statistical Gait Analysis (SGA) and a clustering algorithm that allows for obtaining the muscle principal activations. We evaluated the asymmetry levels of four lower limb muscles in: (1) healthy subjects of different ages (children, adults, and elderly); (2) different populations of orthopedic patients (adults with megaprosthesis of the knee after bone tumor resection, elderly subjects after total knee arthroplasty and elderly subjects after total hip arthroplasty); and (3) neurological patients (children with hemiplegic cerebral palsy and elderly subjects affected by idiopathic Normal Pressure Hydrocephalus). The asymmetry index obtained for each pathological population was then compared to that of age-matched controls. We found asymmetry levels consistent with the expected impact of the different pathologies on muscle activation during gait. This suggests that the proposed index can be successfully used in clinics for an objective assessment of the muscle activation asymmetry during locomotion.**

***Index Terms*— asymmetry, clustering, electromyography, EMG, gait, muscle activation.**

I. Introduction

INSTRUMENTED gait analysis is a powerful method used to quantitatively assess the normal and pathological functions of human walking [1]. The study of EMG cyclic patterns is especially important in the clinical practice and research, as an assessment tool in the management of locomotion pathologies and rehabilitation.

In the last decades, the function of muscles during gait was studied through surface electromyography (sEMG), which allows for determining the timing and extent of muscles activation [2]. However, there is a great variability in sEMG signals collected during gait, even in healthy subjects [3]. To overcome this issue, Statistical Gait Analysis (SGA) was introduced: the acquisition and processing of a large number of gait cycles makes it easier to compare muscles activity of different subjects and to find relevant similarities [4]. Recently, it was proposed an algorithm (CIMAP – Clustering for Identification of Muscle Activation Patterns) [5] and its optimization [6], to further improve SGA. CIMAP enables the grouping of gait cycles into clusters with similar muscle activation patterns [7]. Each cluster is characterized by an element (the prototype) that is representative of all the elements belonging to the cluster. As a spin-off of the CIMAP, the subject's "*principal activations*" can be obtained as the intersection of the cluster prototypes. Principal activations are defined as those muscle activations that are necessary for accomplishing a specific motor task and they describe the essential contributions of a specific muscle to the movement. In recent studies, the extraction of principal activations has proved to be a useful tool for the analysis and interpretation of the muscle activation patterns during gait [8].

In this study we used principal activations to define an index for quantitatively assessing the muscle-activation asymmetry during gait.

Gait asymmetry can be generally defined as the different behavior of the left and right lower limbs during locomotion. The identification of gait asymmetry is very important in the clinical practice, since it may be associated with a number of negative consequences such as inefficiency, difficulty in balance control, risk of musculoskeletal injury to the non-paretic lower limb, and loss of bone mass density in the paretic lower limb [9].

Moreover, pronounced asymmetry levels have been associated with pathological conditions such as cerebral palsy, stroke, osteoarthritis, and knee and hip arthroplasties. Consequently, several different gait asymmetry indexes have been defined in literature [10], [11], [12], [13], helpful for evaluating improvement or deterioration of patient clinical pictures.

However, there is no commonly accepted standard for either the method used to calculate the gait asymmetry or the gait parameters to assess. Most of the studies found in the literature base the asymmetry quantification on spatio-temporal [14], [15] or joint kinematics parameters [16], [17] and only a few studies

C. Castagneri, V. Agostini, S. Rosati, G. Balestra and M. Knaflitz are with the Department of Electronics and Telecommunications, Politecnico di Torino, 10129 Torino, Italy (e-mail: cristina.castagneri@polito.it, valentina.agostini@polito.it,samanta.rosati@polito.it, gabriella.balestra@polito.it, marco.knaflitz@polito.it).

address the problem of defining an asymmetry index based on sEMG signals [18], [19]. To the best of our knowledge, no studies used the extraction of the muscle principal activations obtained from a "physiological" walk as the base to construct a sEMG asymmetry index.

The aim of this work is to define a robust sEMG asymmetry index, for assessing muscle-activation asymmetry in cyclic movements. The proposed index is used to evaluate the asymmetry level of four muscles (Tibialis Anterior, Gastrocnemius Lateralis, Rectus Femoris and Lateral Hamstring) in different populations of healthy controls, as well as in different populations of neurological and orthopedic patients. We also provide a critical comparison with EMG asymmetry indices previously defined in literature [19], [18].

II. Materials and Methods

A. Populations and Gait Data Acquisition

Gait data from a total of 114 subjects were extracted from our database:

(1) 30 control subjects with no neurological or orthopedic pathologies (10 children [4], 10 adults and 10 elderly)

(2) 49 orthopedic patients (19 adults with megaprosthesis of the knee after bone tumor resection (*Mega TKR*), 10 elderly subjects with Total Knee Replacement (*TKR*) and 20 elderly subjects with Total Hip Arthroplasty (*THA*) evaluated at 3, 6 and 12 months after surgery [20])

(3) 35 neurological patients (25 children with Winters' type I and II hemiplegia (*Hemiplegic Children*) after cerebral palsy [21], and 10 elderly subjects with idiopathic Normal Pressure Hydrocephalus (*iNPH*) [22].

Population details are reported in Table I.

The acquisition system STEP32 (Medical Technology, Italy) was used to acquire foot-switch signals and surface EMG signals. Foot-switches (size: 10 mm × 10 mm × 0.5 mm; activation force: 3 N) were placed under the foot-soles, beneath the first and fifth metatarsal heads, and beneath the back portion of the heel. Surface EMG probes were placed over the muscle's belly after skin preparation. EMG signals were acquired from four muscles of both lower limbs: Tibialis Anterior (TA), Gastrocnemius Lateralis (LGS), Rectus Femoris (RF), and Lateral Hamstring (LH). Notice that, since we retrospectively analyzed data collected from previous studies, we selected, for this work, only the common subset of muscles that were present in all of the previous studies. Nevertheless, a pair of agonist-antagonist muscles acting at each joint of the lower limb is present. Active EMG probes were used, with AgCl-disks as electrodes (probe size: 27 mm × 19 mm × 7.5 mm, inter-electrode distance: 12 mm). The signal amplifier had a gain ranging from 1000 to 50000 – adjusted for each specific muscle – and a 3-dB bandwidth from 10 Hz to 400 Hz. The sampling frequency was 2 kHz and signals were converted by a 12-bit analog to digital converter.

Subjects walked barefoot, at self-select speed, back and forth over a straight path (walkway length: from 7 to 15 m, depending on the protocol), for at least 150s.

The experimental protocol conforms to the Helsinki declaration on medical research involving human subjects.

B. EMG signal pre-processing

The SGA routines included in the software of the acquisition system were used to obtain, for each lower limb, the following gait phases: heel contact (H), flat foot contact (F), push off (P), swing (S). The signal was then segmented in separate gait cycles and time-normalized to the stride duration [23]. For all the groups, except for hemiplegic children, we considered only the strides showing the normal sequence of gait phases (H, F, P, S). For hemiplegic children, since a very few numbers of HFPS strides were available, we analyzed the strides of the most represented sequence of gait phases of each subject [21], [24].

A multivariate statistical filter was then used to discard those strides corresponding to the changes of direction along the path (including deceleration before and acceleration after the U-turn) [20].

Finally, for each stride, the ON/OFF muscle activation

TABLE I
POPULATIONS DETAILS

		Number of subjects	Age (mean ± S.D.) [*years*]	Sex	Height (cm) (mean ± S.D.)	Weight (kg) (mean ± S.D.)		Number of analyzed strides (mean ± S.D.)
CONTROLS	*Healthy Children*	10	9 ± 1.5	5M/5F	133.3 ± 7.1	29.1 ± 5.1		164 ± 31
	Healthy Adults	10	39.5 ± 16.2	6M/4F	174.4 ± 9.0	70.4 ± 13.9		197 ± 45
	Healthy Elderly	10	69.7 ± 2.5	5M/5F	167.9 ± 9.1	66.8 ± 12.1		151 ± 20
ORTHOPEDIC PATIENTS	*Megaprosthesis (Mega TKR)*	19	37.8 ± 17.8	10M/9F	170.4 ± 10.5	68.9 ± 11.4		152 ±21
	Total Knee Replacement (TKR)	10	71.2 ± 8.8	5M/5F	168.2 ± 9.1	86.8 ± 21.0		167 ± 29
	Total Hip Arthroplasty (THA)	20	66.1 ± 7.2	11M/9F	168.7 ± 10.5	77.0 ± 13.3	3 m. 6 m. 12 m.	134 ± 19 140 ± 24 159 ± 23
NEUROLOGICAL PATIENTS	*Hemiplegic Children*	25	8.7 ± 3.2	15M/10F	129.7 ± 18.8	30.2 ± 11.7		133 ± 37
	idiopathic Normal Pressure Hydrocephalus (iNPH)	10	72.1 ±9.6	8M/2F	170.8 ± 7.7	78.3 ± 10.5		141 ± 28

intervals were detected by means of a double threshold statistical detector [25].

C. CIMAP algorithm

Considering a specific muscle, at first left and right strides were pooled together (Fig. 1a) and then they were separated in several datasets, grouping strides with the same number of activation intervals (Fig. 1b). Only datasets consisting of at least 35 strides were considered.

We applied dendrogram clustering to every dataset separately. Initially, each stride is considered as a single-element cluster. Then, after each iteration, the two closest clusters are merged, until a unique cluster including all the strides is obtained. A specific cutoff point is used to cut the tree and obtain the final clusterization (see below). The final representative clusters are then obtained considering only those clusters containing at least 10% of the total number of cycles in the dataset (Fig. 1c). Finally, for each representative cluster, left

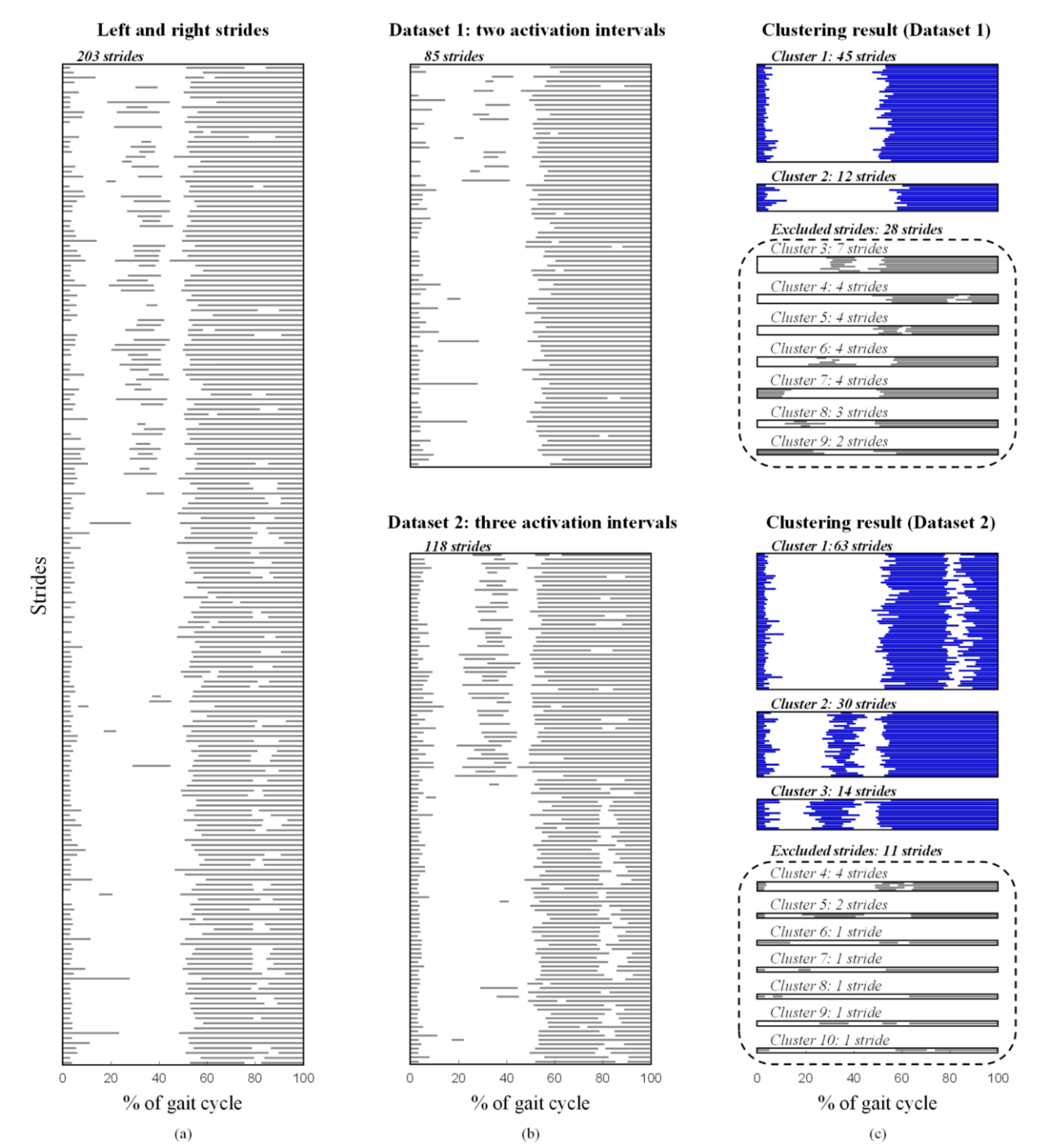

Fig. 1. Example of CIMAP processing pipeline; muscle Tibialias Anterior (TA) of an adult healthy subject. a) Activation intervals of both left and right strides are pooled together. b) Strides are grouped into datasets with the same number of activation intervals. c) Clustering result: strides included in representative clusters are colored in blue, while strides included in not-representative clusters are colored in grey (these are the excluded strides).

and right strides were separated. For each side (left/right), clusters with less than 10% of the original number of strides (of the side under consideration) were discarded. The reason for the exclusion of small clusters (i.e. those containing less than 10% of the total gait cycles) is that their cluster centroids may be misleading if used to characterize the overall activation patterns of the subject.

In a previous work [6] the optimal CIMAP procedure for the dendrogram construction and the stride clusterization was described, considering the following steps detailed below: 1) centroid definition, 2) application of the linkage method, 3) selection of the cutoff point, 4) clustering evaluation.

1) Centroid Definition

The Centroid is the element that characterizes each cluster. In the CIMAP algorithm the centroid was defined as a vector containing the "representative" ON and OFF timings, computed as the median value of the elements belonging to the cluster.

2) Application of the Linkage Method

The Linkage Method is the procedure used to select the clusters to be jointed at each iteration. In our algorithm we applied the complete linkage, which uses the farthest distance between every pair of elements in the two considered clusters as merging criterion [26]. The distance between each couple of clusters corresponds to the distance between those elements (one in each cluster) that are farthest away from each other. At each iteration, the two clusters with the smallest distance are merged together.

To assess the distance during the linkage process we used both the Manhattan and the Chebyshev distance: the dendrograms using both these distances were constructed.

3) Selection of the Cutoff Point

For each dendrogram, we obtained the final clusters using a cutoff rule based on three criteria. We considered the series *Diff* consisting of the differences of inter-cluster distances between two consecutive iterations; then we defined three cutoff points as follows:

- *CutA*: first iteration in which the difference *Diff* is higher than the average difference μ_Diff.
- *CutB:* first iteration in which the difference *Diff* is higher than $\mu\_Diff+\sigma\_Diff$, where σ_Diff is the standard deviation of *Diff*.
- *CutC:* a moving average (window: 5 points) is applied to the *Diff* series. Beginning from the last value and stepping backwards, the cutoff is identified as the point in which the series stop decreasing monotonically.

The best cutoff was identified using (1), which takes into account both the intra-cluster variability and the number of cycles included in the representative clusters:

$$CUT\_IND = \frac{\sum_{i=1}^{n} INTRA\_VAR_i / n}{\sum_{i=1}^{n} |C_i|} \quad (1)$$

where n is the number of representative clusters, $|C_i|$ represents the number of cycles included in each cluster C_i, and $INTRA\_VAR_i$ is the intra-cluster variability of the i-th cluster calculated by using (2):

$$INTRA\_VAR_i = \overline{dist(cycle_j, cycle_k)}, \forall j,k \in C_i \quad (2)$$

where *dist* is the Manhattan distance.

For each dendrogram we computed the three cutoff points and selected the one corresponding to the lowest *CUT_IND* value.

4) Clustering Evaluation

In order to choose the final result, we define an index (*CLUSTER_VAR*) that takes into account two aspects: the similarity between the centroids and the cluster elements, and the number of cycles included in the representative clusters. More specifically, the *CLUSTER_VAR* index, for a single cluster *i*, is calculated by using (3),

$$CLUST\_VAR_i = \sum_{j=1}^{p} dist(cycle_j, CLC_i) / p, \forall j \in C_i \quad (3)$$

where p is the number of cycles included in the representative cluster C_i, CLC_i is the cluster centroid and *dist* represents the Manhattan distance. The final value of *CLUSTER_VAR* is computed as the mean value among all the clusters. The clustering result with the lowest value of the *CLUST_VAR* index was considered as the best result: low values of the index are associated to high intra-cluster similarity and/or high number of cycles included in representative clusters.

D. Principal activation extraction

After clustering, a post-processing phase was performed to extract the principal activations of each muscle. Principal activations are defined as those activations that are necessary for the biomechanical task that is being actuated by the specific muscle [5]. This is complementary to the concept of secondary activations, which are activations present only in some strides and have an auxiliary function in motor control [27] (e.g. to provide a slight correction to muscle activations due to temporary subject distractions or extemporaneous external disturbances).

To extract principal activations, we first defined the cluster prototype as the cluster centroid (Fig. 2a), coded as a string of 1000 elements (0 = no muscle activation; 1 = muscle activation). Then, the principal activation of each muscle was obtained as the intersection of the corresponding cluster prototypes (Fig. 2b). More specifically, principal activations are defined as binary strings of 1000 elements (0 means that at least one prototype has no activation in the specific bit; 1 means that all the prototypes have activation in the specific bit).

E. Muscle-activation asymmetry quantification

For each muscle, we evaluated the muscle-activation asymmetry using an index (*EMG_ASYM_INDEX*), calculated according to (4):

$$EMG\_ASYM\_INDEX = \sum_{i=1}^{N} \frac{|R_i - L_i|}{N} \cdot 100\% \quad (4)$$

where *R* and *L* are the strings corresponding to the principal activations of right and left sides respectively and *N* is the number of elements used for representing the principal activations (*N*=1000). *EMG_ASYM_INDEX* can range from 0% ("perfect" symmetry, the two contralateral muscles are active at the same percent of the gait cycle) to 100% (complete asymmetry, when, with reference to the same percent of the gait cycle, a muscle is active when the contralateral is not).

F. Other EMG indices used in literature

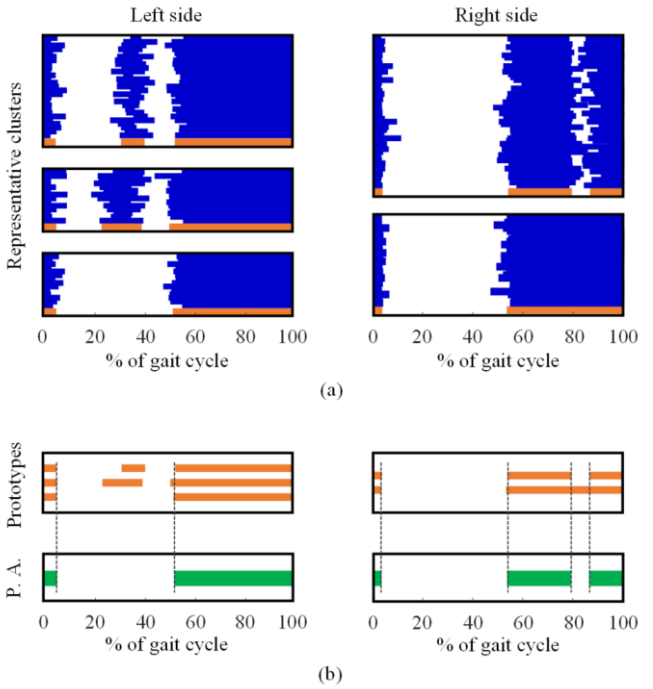

Fig. 2. Example of principal activation (P.A.) extraction for the left and right Tibialis Anterior (TA) muscle of an adult healthy subject. a) Representative clusters: cluster elements (blue), cluster prototypes (orange). b) Principal activations (green), obtained as the intersection of the cluster prototypes.

To compare the proposed index with other indices found in literature, we computed, on our dataset, the asymmetry index (*ASI*) by Schmidt et al. [18] and the symmetry index (SI) by Burnett et al. [19].

In Ref. [18], for each muscle, the EMG envelope is obtained, and *ASI* is defined using (5):

$$ASI(\%) = \left|\frac{2\times(MA_L - MA_R)}{MA_L + MA_R}\right| \times 100\% \quad (5)$$

where MA_L and MA_R represent individual mean muscle activities, obtained during the complete gait cycle of the left and right limb, respectively.

In Ref. [19], for each muscle, *SI* is defined using (6):

$$SI = \frac{RMS_{ND,stance}}{RMS_{D,stance}} \quad (6)$$

where $RMS_{ND,stance}$ and $RMS_{D,stance}$ is the root mean square amplitude during the stance phase for the non-dominant (ND) and dominant (D) limb, respectively. In our dataset, no information was available about the dominant side of subjects. Consequently, we chose to consider as the dominant side:

- the right side, for controls and iNPH patients;
- the sound side, for the remaining groups.

G. Statistical analysis

For each group of subjects detailed in Table I and each muscle, we calculated the mean value and the standard error of the *EMG_ASYM_INDEX*, *ASI* and *SI*.

To explore the differences between patients and healthy controls, we matched each group of patients with one of the three healthy groups (age-based matching). Then, we used the Lilliefors test to assess the normality of the distributions, obtained applying the three indices to our dataset. Because some of the distributions were not normal, the Wilcoxon non-parametric test was used to compare groups ($\alpha = 0.05$), considering each muscle separately. We used 1-tailed tests for *EMG_ASYM_INDEX* and *ASI*, since the mean value of these indices are expected to be higher than (or equal to) that of controls. One-tailed tests were applied also to assess the differences in THA patients during the follow-up (between 3 and 6 months, between 6 and 12 months and between 3 and 12 months). On the other hand, we used 2-tailed tests for the *SI* since, in this case, we could not a-priori hypothesize an effect in one direction, due to definition of the index itself. Indeed, in patients, *SI* may assume values higher or smaller than that of controls, depending on the pathology and the muscle considered.

III. Results and Discussion

Fig. 3 reports the mean values and the standard errors of the *EMG_ASYM_INDEX*, *ASI* and *SI* of the analyzed groups.

A. EMG_ASYM_INDEX

As it emerges from Fig. 3a, overall, we found the lowest values of the index in the three control groups, as it was expected. Moreover, orthopedic and neurological patients show a different behavior depending on the muscle and the type of pathology. The results of the Wilcoxon tests performed to assess the inter-group differences are reported in Table II.

In the following section, we discuss the results that we obtained comparing each group of patients with the corresponding age-matched control group.

We analyzed both orthopedic and neurologic populations in which we expected different levels of asymmetry. More specifically, based on our previous knowledge of the different disorders and treatments which patients underwent:

(1) We expected higher differences between Mega TKR patients and controls with respect to those between TKR patients and controls, since the surgical procedure for the implantation of a megaprosthesis implies a higher degree of bone and muscle sacrifice with respect to that of a conventional prosthesis.

(2) In a previous study, activation patterns of THA patients were analyzed [20]. The results of that study did not evidence substantial (qualitative) differences between prosthetic and

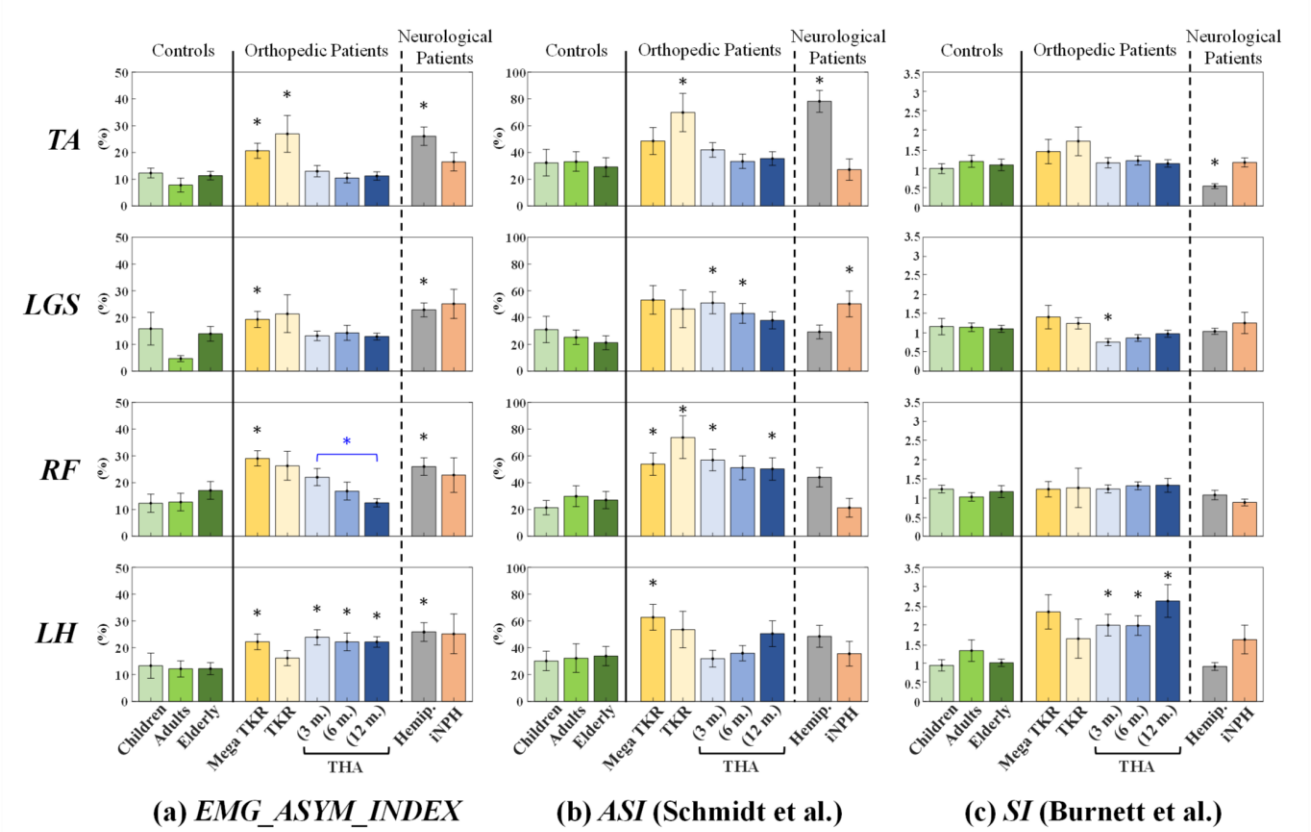

Fig. 3. Mean values and standard errors of (a) *EMG_AYM_INDEX*, (b) *ASI* and (c) *SI* on the analyzed groups. Muscle: Tibialis Anterior (TA), Gastrocnemius Lateralis (LGS), Rectus Femoris (RF) and Lateral hamstring (LH). Significant differences between patients and age-matched controls are marked with a black asterisk. Significant difference between THA patients at 3 and 12 months after surgery is marked with a blue asterisk.

sound sides. Hence, for these patients, we expected a limited asymmetry level in muscle activations.

(3) We also expected different levels of asymmetry on the two groups of neurological patients with respect to controls. In particular, hemiplegia is a condition that affects one side of the body, whereas normal pressure hydrocephalus is not known to selectively affect a specific side.

1) *Mega TKR patients and Healthy Adults*
The Mega TKR group consists of patients affected by malignant tumors of the distal part of the femur, treated through the implant of a modular knee prosthesis (megaprosthesis) for saving their lower limb [28], [29]. This surgical procedure implies different degrees of bone and muscle sacrifice and inevitably leads to a change in the gait characteristics of the prosthetic with respect to the sound side [30]. The EMG_ASYM_INDEX points out this issue clearly: the index values are higher and statistically different in the Mega TKR group with respect to controls for all the four analyzed muscles.

2) *TKR patients and Healthy Elderly*
As explained before, the Total Knee Replacement is less destructive than the megaprosthesis implant; the EMG_ASYM_INDEX reflects this aspect, since index values for TKR patients and controls result significantly different only for the TA muscle.

3) *THA patients and Healthy Elderly*
Patients were evaluated at 3, 6 and 12 months after surgery. The index values for TA, LGS and RF muscles are not significantly different with respect to controls at each time point. On the other hand, LH is the muscle with the greater value of the *EMG_ASYM_INDEX*, and a statistical difference was obtained with respect to healthy elderly at each time point. An interesting behavior is shown by the RF muscle: even if there is no statistical difference respect to the control group, a qualitative decreasing trend can be noted among the three time points. Moreover, the *EMG_ASYM_INDEX* shows a significant difference for this muscle between 3 and 12 months after surgery; this suggests that patients progressively recovered symmetrical muscle activation patterns during walking.

4) *Hemiplegic and Healthy Children*
Hemiplegia is a common consequence of cerebral palsy (CP) and causes altered selective motor control, weakness and spasticity. In a previous study the differences between EMG activation patterns in hemiplegic and healthy children were investigated [21]. Using the defined index, we are also able to identify an asymmetry in muscle activation patterns: the *EMG_ASYM_INDEX* results higher with respect to healthy children, for every muscle.

5) *iNPH patients and Healthy Elderly*
iNPH is a pathology caused by an excess of cerebrospinal fluid in the cerebral ventricles of the brain. This pathology, in many cases, does not affect a specific side of the body,

but it rather affects the overall walking scheme [31]. The results obtained for iNPH patients are consistent with the previous consideration. Differently from what we found for hemiplegic children, we obtained no significant difference with respect to controls.

B. ASI and SI

The results obtained applying the *ASI* and *SI* to our dataset are reported in Fig. 3b and Fig. 3c, respectively. The *p*-values of the Wilcoxon tests are reported in Table II.

We would point out that the *ASI* and *SI* indices found in literature cannot be directly compared to our index *EMG_ASYM_INDEX*. In fact, while both *ASI* and *SI* are related to the mean amplitude of the EMG signal during the whole gait cycle, our index is related to the difference in the EMG onset-offset timings at each percent of the gait cycle. Hence, it provides an information based on the timing of activation patterns rather than EMG amplitudes. Therefore, the information obtained with *EMG_ASYM_INDEX* is complementary with respect to that obtained with *ASI* and *SI*. As an example, using *EMG_ASYM_INDEX* we found differences between hemiplegic children and controls for every muscle. On the contrary, using *ASI* or *SI* we found differences only for the TA muscle. This is reasonable since hemiplegic children are expected to show asymmetric timing patterns in every muscle [21], considering also compensation mechanisms. Moreover, a difference in the mean EMG amplitude asymmetry is observed in the TA muscle considering *ASI* and *SI*. In particular, the *SI* value (smaller than one) highlights a hypoactivation of the TA hemiplegic side with respect to the contralateral one, that confirms findings in literature [32].

IV. Limitations of the Study and Future Works

The CIMAP algorithm relies on a correct identification of the timing of muscular activity. The double threshold algorithm used in the pre-processing stage of the sEMG signals is included in the STEP32 software. However, many detectors of muscular activity have been developed throughout the years, e.g. algorithms that improves SNR estimation in the double threshold detector [33], [34], and algorithms that are based on wavelet-transform [35], [36], or on maximum-likelihood identification [37]. A limitation of this study is that we do not know if the performance of the CIMAP algorithm might be influenced using other pre-processing detection algorithms.

Furthermore, we used the CIMAP to extract principal activations and discard secondary ones. Therefore, the computation of the proposed asymmetry index is based only on principal activations. This aspect, on one side allows for analyzing only those activations that are necessary for the walking task, but, on the other side, it does not allow detecting possible asymmetries lying in secondary activations. In the future, the definition of an asymmetry index including also secondary activation could be introduced.

Moreover, starting from the proposed index, that is specific for each muscle, two aspects can be considered as possible future developments of this study: (1) the definition of a "global" asymmetry index that quantify the overall muscle activity asymmetry; (2) the analysis of possible correlation between foot-floor contact asymmetries and muscle activity asymmetries.

V. Conclusions

In this study we presented an EMG asymmetry index based on principal activations extracted with the CIMAP algorithm.

TABLE II
Comparison between pathological groups and age-matched controls: Wilkoxon-test results

	Group comparison		*EMG_ASYM_INDEX* *p*-values				*ASI (Schmidt et al.)* *p*-values				*(SI) Burnett et al.* *p*-values			
			TA	LGS	RF	LH	TA	LGS	RF	LH	TA	LGS	RF	LH
ORTHOPEDIC PATIENTS	*Mega TKR*	*Healthy Adults*	**0.004**	**0.002**	**0.002**	**0.03**	0.2	0.09	**0.04**	**0.03**	0.9	0.7	1.0	0.3
	TKR	*Healthy Elderly*	**0.03**	0.3	0.1	0.2	**0.02**	0.08	**0.02**	0.2	0.6	0.3	0.2	0.5
	THA 3 months	*Healthy Elderly*	0.5	0.6	0.2	**0.009**	0.1	**0.02**	**0.01**	0.7	1.0	**0.01**	0.4	**0.02**
	THA 6 months	*Healthy Elderly*	0.8	0.6	0.6	**0.01**	0.3	**0.02**	0.07	0.5	0.8	0.1	0.3	**0.004**
	THA 12 months	*Healthy Elderly*	0.5	0.6	0.8	**0.002**	0.2	0.06	**0.04**	0.2	0.8	0.4	0.7	**0.003**
	THA 3 months	*THA 6 months*	0.2	0.5	0.08	0.2	0.1	0.2	0.2	0.8	0.4	0.4	0.4	0.9
	THA 6 months	*THA 12 months*	0.7	0.5	0.3	0.8	0.7	0.4	0.5	0.8	0.9	0.5	0.3	0.4
	THA 3 months	*THA 12 months*	0.3	0.5	**0.01**	0.3	0.2	0.1	0.2	0.9	0.7	0.06	0.8	0.4
NEUROLOGICAL PATIENTS	*Hemiplegic Children*	*Healthy Children*	**0.005**	**0.01**	**0.004**	**0.02**	**0.002**	0.4	0.07	0.2	**0.02**	0.5	0.07	0.9
	iNPH	*Healthy Elderly*	0.08	0.1	0.4	0.1	0.6	**0.01**	0.7	0.5	0.3	0.9	0.5	0.3

Statistically significant differences ($p<0.05$) are highlighted in bold font.

The proposed index is directly based on muscle activity and is not affected by the variability of sEMG patterns since we used only principal activations for its definition.

We quantitatively evaluated the asymmetry levels of four lower limb muscles in healthy subjects and in different populations of orthopedic and neurological patients.

Based on our previous knowledge of the different disorders and treatments which patients underwent, we expected different asymmetry levels on each population. Our results confirmed this expectation. The value obtained for the asymmetry index was consistent with the expected asymmetry level of each specific population of patients. This suggests that the proposed index can be successfully used in clinics for an objective assessment of the asymmetry of muscle activation patterns during locomotion. Furthermore, we would point out that the knowledge provided by our index is complementary to that obtained by means of the other indices found in literature. In fact, it is based on the onset-offset timing of the EMG activation patterns rather than on the mean EMG amplitude.

REFERENCES

[1] T. A. L. Wren, G. E. Gorton, S. Õunpuu, and C. A. Tucker, "Efficacy of clinical gait analysis: A systematic review," *Gait Posture*, vol. 34, no. 2, pp. 149–153, Jun. 2011.

[2] C. Frigo and P. Crenna, "Multichannel SEMG in clinical gait analysis: A review and state-of-the-art," *Clin. Biomech.*, vol. 24, no. 3, pp. 236–245, Mar. 2009.

[3] F. Di Nardo, E. Maranesi, A. Mengarelli, G. Ghetti, L. Burattini, and S. Fioretti, "Assessment of the variability of vastii myoelectric activity in young healthy females during walking: A statistical gait analysis," *J. Electromyogr. Kinesiol.*, vol. 25, no. 5, pp. 800–807, Oct. 2015.

[4] V. Agostini, A. Nascimbeni, A. Gaffuri, P. Imazio, M. G. Benedetti, and M. Knaflitz, "Normative EMG activation patterns of school-age children during gait.," *Gait Posture*, vol. 32, no. 3, pp. 285–9, Jul. 2010.

[5] S. Rosati, V. Agostini, M. Knaflitz, and G. Balestra, "Muscle activation patterns during gait: A hierarchical clustering analysis," *Biomed. Signal Process. Control*, vol. 31, pp. 463–469, 2017.

[6] S. Rosati, C. Castagneri, V. Agostini, M. Knaflitz, and G. Balestra, "Muscle contractions in cyclic movements: Optimization of CIMAP algorithm," in *Proceedings of the Annual International Conference of the IEEE Engineering in Medicine and Biology Society, EMBS*, 2017, pp. 58–61.

[7] V. Agostini, S. Rosati, C. Castagneri, G. Balestra, and M. Knaflitz, "Clustering analysis of EMG cyclic patterns: A validation study across multiple locomotion pathologies," in *2017 IEEE International Instrumentation and Measurement Technology Conference (I2MTC)*, 2017, pp. 1–5.

[8] C. Castagneri, V. Agostini, S. Rosati, G. Balestra, and M. Knaflitz, "Longitudinal assessment of muscle function after Total Hip Arthroplasty : Use of clustering to extract principal activations from EMG signals," *2018 IEEE Int. Symp. Med. Meas. Appl.*, vol. 3528725544, pp. 1–5, 2018.

[9] K. K. Patterson, W. H. Gage, D. Brooks, S. E. Black, and W. E. McIlroy, "Evaluation of gait symmetry after stroke: A comparison of current methods and recommendations for standardization," *Gait Posture*, vol. 31, no. 2, pp. 241–246, 2010.

[10] S. Cabral, R. Fernandes, W. S. Selbie, V. Moniz-Pereira, and A. P. Veloso, "Inter-session agreement and reliability of the Global Gait Asymmetry index in healthy adults," *Gait Posture*, vol. 51, pp. 20–24, Jan. 2017.

[11] E. Auvinet, F. Multon, V. Manning, J. Meunier, and J. P. Cobb, "Validity and sensitivity of the longitudinal asymmetry index to detect gait asymmetry using Microsoft Kinect data," *Gait Posture*, vol. 51, pp. 162–168, Jan. 2017.

[12] J. Heredia-Jimenez, E. Orantes-Gonzalez, and V. M. Soto-Hermoso, "Variability of gait, bilateral coordination, and asymmetry in women with fibromyalgia," *Gait Posture*, vol. 45, pp. 41–44, Mar. 2016.

[13] A. Plate, D. Sedunko, O. Pelykh, C. Schlick, J. R. Ilmberger, and K. Bötzel, "Normative data for arm swing asymmetry: How (a)symmetrical are we?," *Gait Posture*, vol. 41, no. 1, pp. 13–18, Jan. 2015.

[14] K. K. Patterson *et al.*, "Gait Asymmetry in Community-Ambulating Stroke Survivors," *Arch. Phys. Med. Rehabil.*, vol. 89, no. 2, pp. 304–310, Feb. 2008.

[15] K. K. Patterson, A. Mansfield, L. Biasin, K. Brunton, E. L. Inness, and W. E. McIlroy, "Longitudinal Changes in Poststroke Spatiotemporal Gait Asymmetry Over Inpatient Rehabilitation," *Neurorehabil. Neural Repair*, vol. 29, no. 2, pp. 153–162, Feb. 2015.

[16] P. Kutilek, S. Viteckova, Z. Svoboda, and P. Smrcka, "Kinematic quantification of gait asymmetry in patients with peroneal nerve palsy based on bilateral cyclograms.," *J. Musculoskelet. Neuronal Interact.*, vol. 13, no. 2, pp. 244–50, Jun. 2013.

[17] R. L. Lathrop-Lambach *et al.*, "Evidence for joint moment asymmetry in healthy populations during gait," *Gait Posture*, vol. 40, no. 4, pp. 526–531, Sep. 2014.

[18] A. Schmidt *et al.*, "Unilateral hip osteoarthritis: Its effects on preoperative lower limb muscle activation and intramuscular coordination patterns," *Gait Posture*, vol. 45, pp. 187–192, Mar. 2016.

[19] D. R. Burnett, N. H. Campbell-Kyureghyan, P. B. Cerrito, and P. M. Quesada, "Symmetry of ground reaction forces and muscle activity in asymptomatic subjects during walking, sit-to-stand, and stand-to-sit tasks," *J. Electromyogr. Kinesiol.*, vol. 21, no. 4, pp. 610–615, Aug. 2011.

[20] V. Agostini, D. Ganio, K. Facchin, L. Cane, S. Moreira Carneiro, and M. Knaflitz, "Gait parameters and muscle activation patterns at 3, 6 and 12 months after total hip arthroplasty," *J. Arthroplasty*, vol. 29, no. 6, pp. 1265–1272, 2014.

[21] V. Agostini, A. Nascimbeni, A. Gaffuri, and M. Knaflitz, "Multiple gait patterns within the same Winters class in children with hemiplegic cerebral palsy," *Clin. Biomech.*, vol. 30, no. 9, pp. 908–914, Nov. 2015.

[22] V. Agostini *et al.*, "Instrumented Gait Analysis for an Objective Pre-/Postassessment of Tap Test in Normal Pressure Hydrocephalus," *Arch. Phys. Med. Rehabil.*, vol. 96, no. 7, pp. 1235–1241, Jul. 2015.

[23] V. Agostini, G. Balestra, and M. Knaflitz, "Segmentation and Classification of Gait Cycles," *IEEE Trans. Neural Syst. Rehabil. Eng.*, vol. 22, no. 5, pp. 946–952, Sep. 2014.

[24] V. Agostini, M. Knaflitz, A. Nascimberi, and A. Gaffuri, "Gait measurements in hemiplegic children: An automatic analysis of foot-floor contact sequences and electromyographic patterns," in *IEEE MeMeA 2014 - IEEE International Symposium on Medical Measurements and Applications, Proceedings*, 2014.

[25] P. Bonato, T. D'Alessio, and M. Knaflitz, "A statistical method for the measurement of muscle activation intervals from surface myoelectric signal during gait," *IEEE Trans. Biomed. Eng.*, vol. 45, no. 3, pp. 287–299, Mar. 1998.

[26] L. Kaufman and P. J. Rousseeuw, *Finding groups in data : an introduction to cluster analysis*. Wiley-Interscience, 1990.

[27] D. Rimini, V. Agostini, S. Rosati, C. Castagneri, G. Balestra, and M. Knaflitz, "Influence of pre-processing in the extraction of muscle synergies during human locomotion," in *Proceedings of the Annual International Conference of the IEEE Engineering in Medicine and Biology Society, EMBS*, 2017, pp. 2502–2505.

[28] R. P. H. Veth, R. van Hoesel, M. Pruszczynski, J. Hoogenhout, B. Schreuder, and T. Wobbes, "Limb salvage in musculoskeletal oncology," *Lancet Oncology*, vol. 4, no. 6. Elsevier, pp. 343–350, Jun-2003.

[29] S. Höll *et al.*, "Distal femur and proximal tibia replacement with megaprosthesis in revision knee arthroplasty: a limb-saving procedure," *Knee Surgery, Sport. Traumatol. Arthrosc.*, vol. 20, no. 12, pp. 2513–2518, Dec. 2012.

[30] A. Kawai, S. I. Backus, J. C. Otis, H. Inoue, and J. H. Healey, "Gait characteristics of patients after proximal femoral replacement for malignant bone tumour.," *J. Bone Joint Surg. Br.*, vol. 82, no. 5, pp. 666–9, 2000.

[31] N. R. Graff-Radford, "Normal Pressure Hydrocephalus," *Neurol. Clin.*, vol. 25, no. 3, pp. 809–832, Aug. 2007.

[32] T. F. Winters, J. R. Gage, and R. Hicks, "Gait patterns in spastic

hemiplegia in children and young adults.," *J. Bone Joint Surg. Am.*, vol. 69, no. 3, pp. 437–41, Mar. 1987.

[33] G. Severini, S. Conforto, M. Schmid, and T. D'Alessio, "Novel formulation of a double threshold algorithm for the estimation of muscle activation intervals designed for variable SNR environments," *J. Electromyogr. Kinesiol.*, vol. 22, no. 6, pp. 878–885, 2012.

[34] G. Severini, S. Conforto, C. De Marchis, M. Schmid, and T. D'Alessio, "A SNR-independent formulation of a double threshold algorithm for the estimation of muscle activation intervals," *Proc. Annu. Int. Conf. IEEE Eng. Med. Biol. Soc. EMBS*, no. 1, pp. 7500–7503, 2011.

[35] G. Vannozzi, S. Conforto, and T. D'Alessio, "Automatic detection of surface EMG activation timing using a wavelet transform based method," *J. Electromyogr. Kinesiol.*, vol. 20, no. 4, pp. 767–772, 2010.

[36] T. Varrecchia, C. D'Anna, A. Scorza, S. A. Sciuto, and S. Conforto, "Muscle activity detection in pathological, weak and noisy myoelectric signals," *MeMeA 2018 - 2018 IEEE Int. Symp. Med. Meas. Appl. Proc.*, pp. 1–5, 2018.

[37] Q. Xu, Y. Quan, L. Yang, and J. He, "An adaptive algorithm for the determination of the onset and offset of muscle contraction by EMG signal processing," *IEEE Trans. Neural Syst. Rehabil. Eng.*, vol. 21, no. 1, pp. 65–73, 2013.